

Dynamic Stress Changes during Earthquake Rupture

by Steven M. Day, Guang Yu, and David J. Wald

Abstract We assess two competing dynamic interpretations that have been proposed for the short slip durations characteristic of kinematic earthquake models derived by inversion of earthquake waveform and geodetic data. The first interpretation would require a fault constitutive relationship in which rapid dynamic restrengthening of the fault surface occurs after passage of the rupture front, a hypothesized mechanical behavior that has been referred to as “self-healing.” The second interpretation would require sufficient spatial heterogeneity of stress drop to permit rapid equilibration of elastic stresses with the residual dynamic friction level, a condition we refer to as “geometrical constraint.” These interpretations imply contrasting predictions for the time dependence of the fault-plane shear stresses. We compare these predictions with dynamic shear stress changes for the 1992 Landers (M 7.3), 1994 Northridge (M 6.7), and 1995 Kobe (M 6.9) earthquakes. Stress changes are computed from kinematic slip models of these earthquakes, using a finite-difference method. For each event, static stress drop is highly variable spatially, with high stress-drop patches embedded in a background of low, and largely negative, stress drop. The time histories of stress change show predominantly monotonic stress change after passage of the rupture front, settling to a residual level, without significant evidence for dynamic restrengthening. The stress change at the rupture front is usually gradual rather than abrupt, probably reflecting the limited resolution inherent in the underlying kinematic inversions. On the basis of this analysis, as well as recent similar results obtained independently for the Kobe and Morgan Hill earthquakes, we conclude that, at the present time, the self-healing hypothesis is unnecessary to explain earthquake kinematics.

Introduction

In recent years, extensive sets of high-quality, near-source strong-motion recordings have become available from a number of large earthquakes. Interpretation of multi-station strong-motion data sets, often in combination with data from geological mapping of surface offsets, geodetic observations of static deformation, and/or teleseismic waveforms, has greatly expanded our understanding of the geometry and kinematics of earthquake rupture. Rather detailed space-time images of the earthquake rupture process have been constructed through the fitting of these data to kinematic models. Sometimes model construction has been by trial-and-error search of a model space (e.g., Archuleta, 1984). More commonly, a parameterization has been employed in which the data are linear functionals of the model parameters, permitting model construction by direct solution of a linear system (e.g., Olson and Apsel, 1982; Hartzell and Heaton, 1983). Some studies have employed less restrictive model parameterizations, using linearized inversion (e.g., Beroza and Spudich, 1988; Cotton and Campillo, 1995) or nonlinear optimization (e.g., Zeng and Anderson, 1996; Hartzell *et al.*, 1996) for model construction.

One fundamental purpose of these kinematic inversions is to reveal elements of the physical processes operating on faults during earthquakes. A step toward that end is the estimation of a few dynamic parameters of the earthquake. The inference of dynamic parameters from kinematic models is usually accomplished with the aid of shear crack models of faulting. For example, shear crack models have been used as the basis for inferring various measures of earthquake stress drop, given a kinematic characterization of the faulting. Shear crack models have also been used to estimate the fracture strength associated with breakdown processes at the earthquake rupture front (e.g., Rice, 1996).

Likewise, simple crack models have been invoked to infer the physical process arresting sliding on the fault surface after it has ruptured. In this case, a key kinematic parameter is the slip rise time, or duration (we will use the terms interchangeably). By slip duration, we mean the time between rupture arrival at a point on the fault surface and cessation of sliding at that same point. The *slip* duration is thus distinct from the overall *source* duration. By simple crack models, we mean models in which (1) conditions of

prestress and frictional strength are spatially uniform and (2) the post-failure crack surface has an approximately constant residual level of sliding friction. The latter criterion is met, for example, by crack models with slip-weakening constitutive relationships (e.g., Ida, 1972; Andrews, 1976; Day, 1982a). Madariaga (1976) showed that slip duration on equidimensional shear cracks is approximately equal to the ratio of fault radius to S -wave speed. Day (1982b) showed that the duration of slip in high aspect ratio shear cracks is approximately equal to half the ratio of the shorter dimension of the fault surface to the rupture velocity.

In contrast, most earthquake kinematic inversions indicate that slip duration is substantially shorter than the simple crack-model predictions. For example, Heaton (1990) reviewed kinematic earthquake models derived from waveform modeling of seven earthquakes and noted that the inferred slip durations were significantly shorter than the expected duration. Most subsequent studies have also yielded slip duration estimates significantly shorter than would be expected from the overall fault dimensions, although in at least some cases, it is uncertain whether the distinction is resolvable with available data (e.g., Cotton and Campillo, 1995).

Another way of stating this relationship between slip duration and fault dimension is that only a relatively small fraction of the overall fault surface, a strip immediately behind the rupture front, is actively sliding at any given instant. This mode of faulting has therefore been referred to as a "propagating slip pulse." This slip-pulse behavior contrasts with the behavior of simple propagating shear cracks undergoing uniform stress drop. In crack models in which the final crack surface is roughly equidimensional, nearly the entire crack surface is actively sliding during much of the rupture process. In long, narrow, shear crack models, with narrow dimension of length w , slip does form a propagating pulse; however, the active portion of the fault encompasses a strip extending a distance of roughly $w/2$ behind the rupture front, apparently too wide a slip pulse, at least in some cases, to be consistent with kinematic inversion results. Archuleta and Day (1980, Fig. 5) show an example of this propagating pulse behavior in a simulation of a long, narrow, surface-rupturing earthquake.

This article examines two competing dynamic interpretations that have been proposed for the short slip durations characteristic of kinematic earthquake models. One interpretation holds that the predominant mechanism arresting slip at a point on the fault surface is a frictional strength increase induced dynamically at that point as an inherent part of the local constitutive functional relating frictional strength to the slip history. This is the so-called "self-healing" hypothesis. The alternative interpretation assumes a simpler frictional behavior, analogous to that observed in most frictional sliding experiments in rock, in which post-rupture frictional strength remains roughly constant on the timescale associated with stick-slip events. In this interpretation, the arrest of slip at a point is predominantly the result of that point

attaining equilibrium with the surrounding continuum at this residual dynamic friction level. Short slip duration then results when the time to equilibrium is short, as a result of spatial heterogeneity of the stress drop.

These two interpretations differ fundamentally in their predictions for the time dependence of shear stress changes accompanying slip. We therefore examine the shear stress changes implied by the kinematic images previously obtained for recent, well-recorded earthquakes and compare these stress-change functions to the model predictions. The events analyzed are the 1992 Landers, California, earthquake (M 7.3), the 1994 Northridge, California, earthquake (M 6.7), and the 1995 Kobe, Japan, earthquake (M 6.9). We find that there is little or no actual evidence for self-healing friction in kinematic inversion results. The self-healing concept appears to be unnecessary for explaining the observed propagating slip pulses. Ide and Takeo (1997) have performed analogous computations for one of the events examined here (the 1995 Kobe earthquake), using a similar computational approach. They also conclude that the Kobe earthquake is consistent with a constitutive relation of slip-weakening type, which does not show self-healing behavior.

It is well known that seismic directivity associated with propagating slip pulses can generate intense ground-velocity transients in the near-source region of earthquakes. We emphasize that the occurrence of these large-velocity pulses, and the significant hazard associated with them, is not in question in this article. We address only the physical mechanism giving rise to the slip pulse mode of rupture.

Background

The apparent discrepancy noted in the Introduction between simple crack models and earthquake kinematic reconstructions from waveform fitting has received much attention and has led to speculation that the kinematic inversions might be revealing some previously unrecognized mode of frictional behavior. To explain the short slip durations, Heaton (1990) proposed that frictional resistance on a fault, after dropping to a dynamic friction level at the time of rupture, undergoes a rapid increase, or strength recovery, after passage of the rupture front. This dynamic restrengthening of the fault would arrest sliding sooner than would occur if the fault strength remained at a constant dynamic friction level after rupture. The dynamic restrengthening behavior could be modeled phenomenologically by introducing a friction coefficient with an inverse proportionality to slip velocity. Several authors (e.g., Perrin *et al.*, 1996; Cochard and Madariaga, 1996; Beeler and Tullis, 1996) have shown theoretically that, for certain parameter ranges, friction laws with velocity-dependent friction can give rise to propagating slip pulses.

Heaton (1990) called this hypothesized behavior "self-healing." Following Heaton (1990), we will restrict the term "self-healing" to refer to behavior in which rapid restrengthening of the fault accounts for the arrest of sliding behind

the rupture front. The term thus refers to this particular physical explanation for the observed slip pulse behavior, not to the slip pulse behavior itself. The term “healing,” without a modifier, will be used to indicate cessation of slip, without implications as to the causative mechanism. As noted by Heaton, there are a number of more or less plausible mechanisms that may be capable of providing an underlying physical basis for self-healing behavior. Among the candidate mechanisms that have been cited are acoustic fluidization (Melosh, 1979), fault-normal stress perturbations (Brune *et al.*, 1993; Andrews and Ben-Zion, 1996; Harris and Day, 1997), and rapid dissipation of elevated pore fluid pressures induced by shear heating near the rupture front (Sibson, 1973; Lachenbruch, 1980).

At the present time, laboratory experiments on rock do not provide any independent evidence for the existence of the self-healing mode of friction. Figure 1, for example, illustrates the frictional behavior measured in simulated earthquakes in two different laboratories. Figure 1a shows slip and shear stress measurements obtained by Dieterich (1981) following spontaneous nucleation of a slick slip event on a pre-cut interface in a 1.5-m-square slab of granite. Shear stress drops to a dynamic friction level upon passage of the rupture front and remains near that level throughout the event. Arrest of sliding appears to occur when the system reaches equilibrium at or below this frictional resistance level, not as a result of dynamic restrengthening. Figure 1b shows some results from a similar experiment by Ohnaka and Kuwahara (1990). Again, frictional stress remains low following the drop in stress at the rupture front. In both cases, the shear stress has considerable small-scale complexity, but no systematic restrengthening suggestive of self-healing accompanies the cessation of slip. These observations should not be taken as evidence against a self-healing mechanism operating during earthquakes, as we cannot confidently scale the laboratory results to the dimensions of crustal faulting. Rather, our point is to emphasize the absence of independent positive evidence, currently, for rock mechanical behavior of this type.

An alternative mechanism to account for early cessation of slip is geometrical in origin: the well-known spatial heterogeneity of slip in large earthquakes. Kinematic inversions reveal that areas of large slip usually comprise only a small fraction of the total area that ruptures in a large earthquake. Thus, the high slip regions have characteristic length scales smaller than those of the overall rupture surface. Therefore, we would expect a reduced time for these areas to reach equilibrium with the dynamic frictional stresses, without necessarily invoking any enhanced (i.e., relative to laboratory measurements) velocity dependence of friction or other form of rapid strength recovery behind the rupture front.

This latter model, in which reduced slip duration results from geometrical constraints on the high stress-drop areas, over length scales smaller than the overall fault dimension, we will refer to as the “geometrical constraint” model. Mikumo (1994) has explored this idea that the dimensions of

pre-existing stress and/or strength heterogeneities on the fault plane might provide adequate geometrical constraint to explain short rise times of slip. Mikumo’s dynamic shear crack models demonstrate the plausibility of this model as a cause of short slip durations. Mikumo and Miyatake (1995) have derived static stress-drop distributions for the 1984 Morgan Hill, California, earthquake that are compatible with the heterogeneous static slip distribution evident from the kinematic waveform inversion of Beroza and Spudich (1988). Fukuyama and Mikumo (1993) developed an iterative inversion method for fitting waveform data to dynamic crack models with heterogeneous stress drop and strength. Using a similar method, Beroza and Mikumo (1996) have demonstrated that a dynamic model with spatially variable stress drop and strength, but without any self-healing mechanism, can explain the seismic observations of the 1984 Morgan Hill earthquake at least as well as published kinematic models.

Figure 2 shows, schematically, the contrasting predictions of the self-healing and geometrical constraint models for shear stress, as a function of time, at a representative point on the fault surface. In both cases, shear stress drops abruptly as the rupture front passes. The subsequent behavior, however, differs. The self-healing model requires a pronounced recovery of shear stress during the process of slip, with the shear stress at the time of healing being well above the minimum value reached right behind the rupture front. The geometrical constraint model predicts shear stress histories on the fault that fall to a roughly constant residual dynamic friction level after passage of the rupture front, and subsequently remain at or below that level. Examples of the behaviors sketched qualitatively in Figure 2 can be seen in the numerical simulations of Cochard and Madariaga (1996, Fig. 16).

Two points of clarification are necessary regarding Figure 2. First, the figure shows very similar slip pulses for the two models, but very different shear stress histories. Naturally, this difference is only possible if the slip in at least one of the two models is spatially variable (and, of course, spatial variability is implicit in the geometrical constraint model). Second, Figure 2 is only meant to describe behavior at a representative point of the fault plane. As Cochard and Madariaga (1994, 1996) point out, self-healing frictional models may induce strong heterogeneities in the final stress, with the result that the stress recovery phase of Figure 2a may not be apparent at every fault point.

The two models are, of course, end members of a set of possible models combining both types of behavior. The end-member models have differing implications for fault dynamics, as Heaton (1990) has discussed. In the self-healing model, rather than the heterogeneity of the fault-zone initial conditions controlling the slip duration and distribution, nonlinear dynamics of the slip process would be dominant. Since healing, in this model, is controlled by local dynamic processes, the global behavior of the rupture might be largely a consequence of complex dynamical effects occurring near

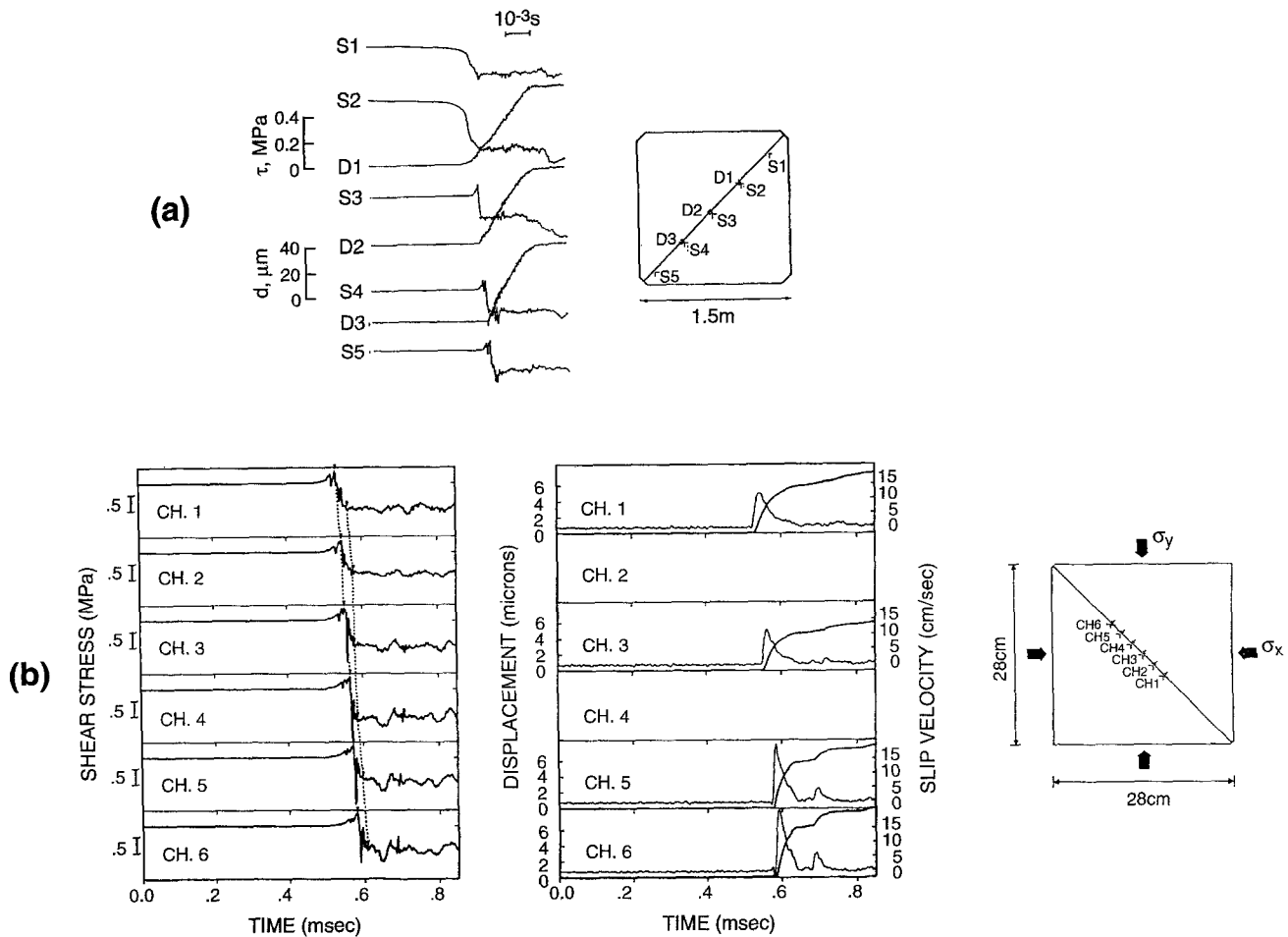


Figure 1. Slip and shear stress time histories from stick-slip laboratory experiments on precut faults: (a) Results of Dieterich (1981) for an event in a $1.5 \times 1.5 \times 0.4$ m granite slab under normal stress of 1.4 MPa. Stress traces are labeled S1–S5, slip displacement traces are labeled D1–D3. (b) Results obtained by Ohnaka and Kuwahara (1990) for an event in a $20 \times 20 \times 5$ cm granite slab. Shear stress records are on the left; slip displacement and velocity, on the right.

the rupture front. In this conceptual picture, the subsequent progress of rupture might be highly unpredictable, even with considerable foreknowledge of the initial conditions of the fault zone. This general expectation is substantiated by the earthquake simulations of Cochard and Madariaga (1996), which postulated a self-healing fault rheology (modeled via a strongly velocity-dependent friction coefficient). Those simulations demonstrated that complex rupture characteristics can emerge spontaneously in this case, even under uniform initial conditions. In contrast, if the geometrical constraint model is more appropriate, pre-existing geological and mechanical features of the fault zone, in conjunction with the fault's previous heterogeneous slip history, would provide the geometrical barriers and stress concentrations that could be expected to provide the predominant controls on rupture evolution.

As noted earlier, we have little or no independent evidence from laboratory friction experiments to support a self-healing fault rheology. The self-healing concept has devel-

oped primarily to explain the slip histories of earthquakes. Thus, it is appropriate to test whether such self-healing behavior is actually required in a dynamic interpretation of those same slip histories. To do so, we calculate the shear stress change, as a function of time and position on the fault surface, implied by kinematic models of several recent earthquakes. We then compare the stress-change time functions with the characteristic behaviors shown in Figure 2.

Method of Analysis

Our starting point is a set of kinematic images, that is, inferred slip velocity as a function of fault-plane coordinate and time, for three recent, large crustal earthquakes. Combinations of strong-motion, teleseismic, and geodetic data were used to develop these images of fault slip. The kinematic models considered here are those for the 1992 Landers, California, M 7.3 earthquake (Wald and Heaton, 1994), the 1994 Northridge, California, M 6.7 earthquake (Wald *et*

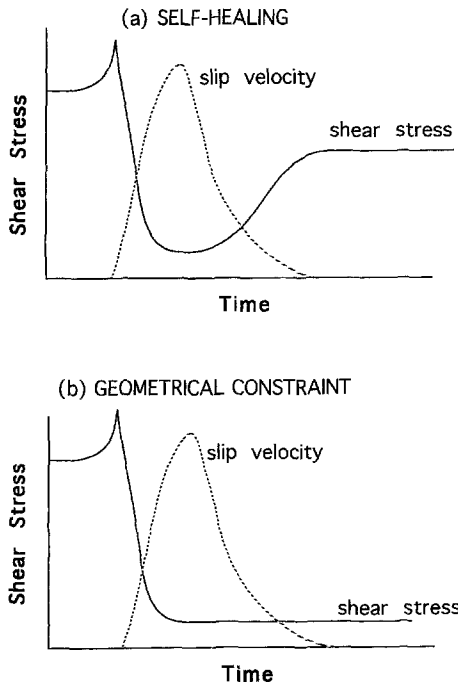


Figure 2. Characteristic shear stress time histories for (a) self-healing and (b) geometrical constraint models for slip duration.

al., 1996), and the 1995 Kobe, Japan, M 6.9 earthquake (Wald, 1996).

We examine the time-dependent changes in fault-plane shear stress implied by the slip model of each earthquake. This is done in two stages. The first stage is interpolation and smoothing to convert the slip model to a continuously differentiable slip-rate function of fault-plane position ξ and time t , $\dot{s}(\xi, t)$. The second stage is computation of the shear stress changes, $\Delta\tau(\xi, t)$, from $\dot{s}(\xi, t)$.

Interpolation and Smoothing. The original Wald *et al.* kinematic models parameterize the slip rate in the following manner. The fault surface is specified *a priori* and partitioned into N_ξ nonoverlapping rectangular elements. The slip-rate time function is the sum of N_t propagating pulses of triangular shape and width Δt_1 , $W(t/\Delta t_1)$, each of which travels with the same, constant, velocity V_r , starting from a prescribed hypocentral location, with delay Δt_2 between consecutive triangular pulses. The amplitude of each propagating pulse is a piecewise constant function of fault-plane position, constant over each partition of the fault. Thus, the original slip-rate function has the form

$$\dot{s}(\xi, t) = \sum_{n=0}^{N_t-1} \mathbf{A}_n(\xi) W[(t - R/V_r - n\Delta t_2)/\Delta t_1],$$

where \mathbf{A}_n , $n = 0, \dots, N_t - 1$, are N_t piecewise constant, two-component vector functions of position, and R is the

hypocentral distance of the point ξ . The fault dimensions, hypocentral location, triangular pulse width Δt_1 , number of pulses N_t , pulse delay Δt_2 , and the window velocity V_r , are all specified *a priori*. The $2N_\xi N_t$ scalar constants defining the \mathbf{A}_n s are obtained by optimizing the fit to seismic and other data.

Prior to doing the stress computations, we convert the discontinuous slip rate, $\dot{s}(\xi, t)$, to a continuous function of space and time, $\hat{s}(\xi, t)$, by interpolation and smoothing. First, we interpolate each piecewise constant amplitude function \mathbf{A}_n biquadratically from its values at the partition centers, generating a continuous amplitude function. Then, we smooth the time function $W(t)$ by taking a running mean, with averaging width equal to the triangular pulse duration Δt_1 . This removal of discontinuities is justified by the fact that the slip images were derived using only relatively long-wavelength observations. In addition to the static (geodetic) observations, only seismic observations with period longer than 1 sec (Northridge) or 2 sec (Landers and Kobe) were used to derive the kinematic models used for this study.

Computation of Shear Stress Change Function. The second stage of the analysis is determination of the shear stress changes that are implied by the kinematic models. Assuming that linear elastodynamics governs the disturbance off the fault plane itself (and that initial velocities are everywhere zero, and no other sources act), knowledge of the slip function everywhere on the fault plane determines the stress-change time history everywhere on the fault. If it were adequate to approximate the continuum surrounding the fault as being uniform and unbounded, then we could conveniently write the shear stress change as a surface and time integral of the product of the slip function and Green's tensor (e.g., Fukuyama and Madariaga, 1995; Bouchon, 1997). A surface and time integration is then required to evaluate the stress at each fault plane point of interest and each time history point (though Fourier methods can be used to reduce the computation considerably, due to the translational symmetry of the continuum that was assumed). When material interfaces and the free surface are considered, the integral formulation for stress is still possible in principle, but evaluation of Green's tensor becomes computationally intensive, and the integral approach is not attractive. In either case, direct time stepping of the elastodynamic equations by a volume discretization method such as the finite-difference method is a straightforward alternative and provides the most practical method of solution in the latter case.

Here, we use a finite-difference method to compute a space-time image of the coseismic shear stress changes for each of the events studied. The volume discretization is three dimensional, time integration is explicit, and spatial and temporal accuracy are second order. The fault is represented using surfaces containing double nodes, and the function $\hat{s}(\xi, t)$ is discretized and applied as a velocity jump condition between double nodes. Multiple, noncoplanar discontinuity surfaces (Harris *et al.*, 1991; Harris and Day, 1993) are also

included in this way, in order to treat segmented fault ruptures such as the Landers and Kobe events.

Landers Model. Details of the Landers kinematic inversion are given by Wald and Heaton (1994). The resulting model represents the fault system by 186 subdomains of uniform slip on three fault segments, a Landers/Johnson Valley (LJV) segment (30 km long), Homestead Valley (HV) segment (27 km long), and Camprock/Emerson (CE) segment (36 km long), respectively. All segments extend from the surface to 15 km depth. To simplify the stress computations, we neglect the changes in strike among the three segments, but we do incorporate 1-km right steps between the LJV and HV segments and between the HV and CE segments. We also simplify the earth model of Wald and Heaton to a uniform half-space (wave speeds 6.2 and 3.52 km/sec and density 2.7 gm/cm³). We interpolate the slip function onto 5580 double-node points on a uniform grid with 0.5-km internode spacing and smooth the slip time history with a 1-sec running mean.

Northridge Model. Details of the Northridge kinematic inversion are in Wald *et al.* (1996). There are 196 uniform-slip subdomains on a single fault plane (dimensions 18 km along strike, 24 km down-dip), which we interpolate onto 6912 double-node points on a uniform grid with 0.25-km node spacing. Since the fault plane is quite deeply buried, never reaching within 6 km of the Earth's surface, we simplify the stress computations in this case by neglecting both geologic stratification and the free-surface boundary condition, performing the stress computations for a uniform whole space (wave speeds 6.3 and 3.6 km/sec, density 2.8 gm/cm³). The smaller node spacing in this case corresponds to the fact that the Wald *et al.* inversions used strong-motion data up to 1 Hz, in contrast to the upper cutoff of 0.5 Hz used in the Landers and Kobe inversions. We smooth the Northridge slip time history with a 0.6-sec running mean. The shorter time-domain smoothing interval for the Northridge model, compared with Landers, corresponds to the shorter time windows used in the kinematic inversion.

Kobe Model. Details of the Kobe kinematic inversion are given by Wald (1996). The model contains 144 uniform-slip subdomains on two subparallel fault segments, the Nojima (20 km long) and Suma/Suwayama (40 km long) segments. The faults extend from the surface to 20 km depth. To simplify the stress computations, we neglect the 5° strike difference between the segments and the 5° and 10° departures of the fault planes from the vertical. The earth model was a layer (wave speeds 5.5 and 3.2 km/sec, density 2.6 gm/cm³) over a uniform half-space (wave speeds 6.0 and 3.46 km/sec, density 2.7 gm/cm³), somewhat simplifying the multi-layer model of Wald. We included a 0.5-km right step between the segments (a smaller stepover than that assumed in Wald's model, though the difference has little effect on the results). The slip function was interpolated onto 4800 double-node points on a uniform grid of 0.5-km spacing, then

temporally smoothed by a 0.7-sec running mean, the smoothing time again corresponding to the length of the time windows employed in the kinematic inversion.

Results

Figure 3 shows the inferred static shear stress change (with stress *drops* shown as positive numbers) for the three earthquake models. For Landers and Kobe, we show the component of shear stress change in the strike direction, and for Northridge, we show shear stress change resolved onto the up-dip direction. The three segments of the Landers earthquake model are in Figure 3a. The color map has been adjusted so that regions of stress increase (i.e., negative stress drop) are blue. The static stress drop is highly variable spatially. Small patches of large, positive stress drop, sometimes exceeding 60 MPa, occur in the model. These are surrounded by patches where coseismic shear stress undergoes either a very small drop or an increase, the stress increases sometimes exceeding 20 MPa. Since we do not know the initial stress state, we do not know whether the heterogeneity of the stress drop is primarily a consequence of heterogeneity in the initial stress state, heterogeneity of the final stress state (e.g., due to heterogeneity of the strength drop), or some complex combination of the two.

It is doubtful that the extreme values in Figure 3a are actually resolvable, since the original kinematic models are constrained only by relatively long wavelength seismic data, with the 0.5-Hz cutoff corresponding to roughly a 6-km *S* wavelength. However, resolution limitations would not appear to compromise the general picture of highly localized high stress drops largely contained in a low or negative stress-drop background. In any event, it is not necessary to confront the question of resolution in order to address our primary objective, which is to test whether the observations, and the kinematic models that have been fit to them, require a self-healing hypothesis.

The inferred shear stress changes, as a function of time, are shown for each of the three Landers model segments in Figures 4a, 4b, and 4c, respectively. The stress-change time histories are shown for each of a grid of points on each fault, with the location of the left edge of each curve indicating the location of that grid point. Stress change is positive up in these figures, so that the curves are deflected downward for positive stress drops. On those parts of the faults where slip is large, and therefore likely to be well resolved, the inferred stress-drop time dependence is invariably monotonic after passage of the rupture front. Thus, Figure 4 is consistent with the geometrical constraint hypothesis. A plausible interpretation is that the low (often negative) stress-drop zones provide sufficient geometrical constraint to the slip process to arrest sliding, limiting the duration of the slip pulses. In the high-slip regions of Figure 4, for which the slip model is relatively well constrained by the observations, there is no evidence of the dynamic restrengthening

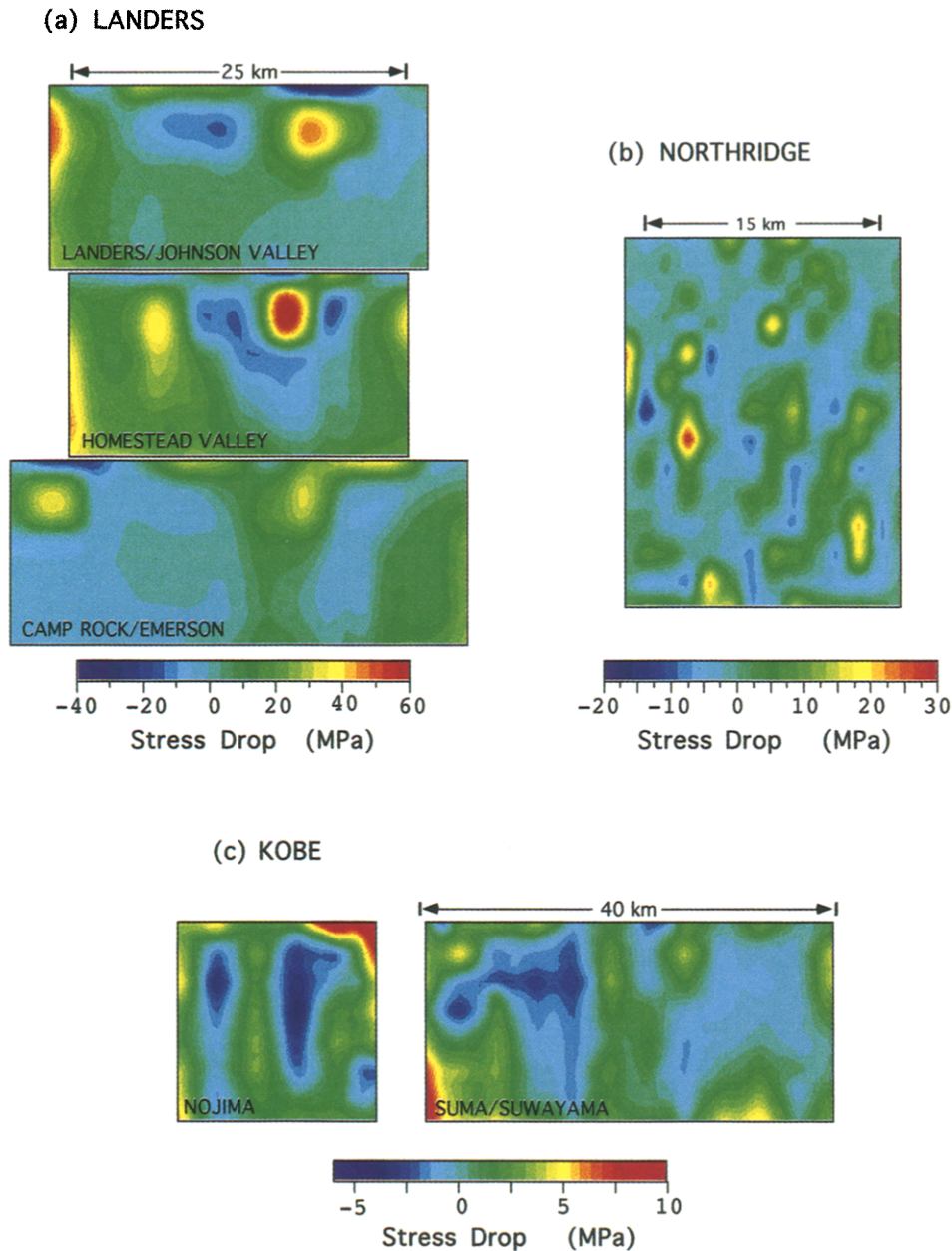


Figure 3. Static stress drop calculated for kinematic models of the three earthquakes analyzed. In each case, blue hues indicate negative stress drop. (a) Landers earthquake, (b) Northridge earthquake, and (c) Kobe earthquake.

(see Fig. 2) that is the defining characteristic of a self-healing fault-zone rheology. In some low-slip areas, such as on the lower half of the LJV segment, near its along-strike center, there is some indication of overshoot in the shear stress, though this may simply reflect poorer resolution in the low-slip areas.

Figure 3b shows the static shear stress change inferred for the Northridge earthquake. As in Figure 3a, the color map has been adjusted so that negative stress drops appear in blue. This time the pattern of localized regions of high stress drop confined in a negative stress-drop background is even more striking. Local stress-drop maxima exceed 40

MPa in Figure 3b, though, as before, these maxima are unlikely to be resolvable from the data employed. Bouchon (1997) also computed the Northridge static stress drop from the Wald *et al.* kinematic model. While Bouchon's results differ from ours in detail, they show a very similar overall pattern. The differences are probably a result of differences in the smoothing schemes applied to the kinematic model. Figure 5 shows the shear stress-change time histories inferred for Northridge. As was the case for Landers, the stress changes are predominantly monotonic after passage of the rupture front, with little, if any, indication of self-healing. As was the case for Landers, the behavior is clearly consis-

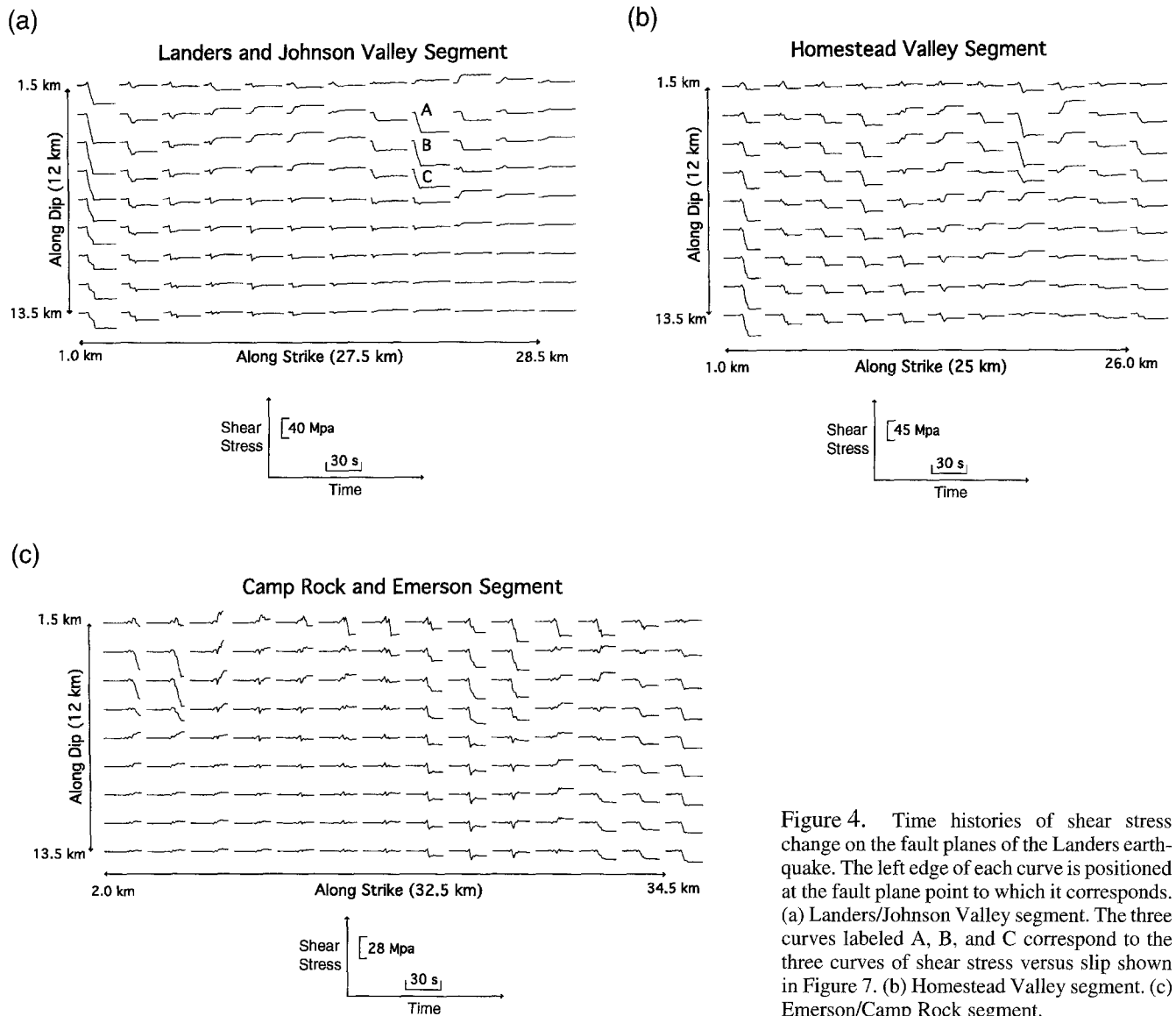


Figure 4. Time histories of shear stress change on the fault planes of the Landers earthquake. The left edge of each curve is positioned at the fault plane point to which it corresponds. (a) Landers/Johnson Valley segment. The three curves labeled A, B, and C correspond to the three curves of shear stress versus slip shown in Figure 7. (b) Homestead Valley segment. (c) Emerson/Camp Rock segment.

tent with healing due to equilibration with a roughly constant residual dynamic frictional stress.

Static shear stress changes for Wald's two-segment model of the Kobe earthquake are shown in Figure 3c, again showing a pattern of high stress-drop regions confined in a low or negative stress-drop background. A large percentage of the fault area shows negative stress drop, corresponding to the large patches of zero or near-zero slip in the Wald kinematic model. Figures 6a and 6b show the corresponding time histories for the Suma/Suwayama and Nojima segments, respectively. As was the case for the other two events, the stress time histories are consistent with geometrical control of slip duration. The only time histories perhaps suggestive of self-healing are located at the south end of the Suma/Suwayama segment near the bottom edge of the fault surface. Were slip duration in the Kobe model controlled primarily by a self-healing rheology, we would expect this signature to dominate the stress time histories in these figures, which it clearly does not.

Discussion

The dynamic analysis previously described indicates that the self-healing hypothesis is unnecessary to explain the inferred slip durations in these earthquakes. The earthquakes analyzed were from a range of tectonic environments, and each was particularly well recorded by strong-motion, teleseismic, and geodetic networks. For the Kobe earthquake, the same conclusion was derived from a similar analysis by Ide and Takeo (1997). Applying a somewhat different analytical approach, Beroza and Mikumo (1996) reach a similar conclusion for the 1984 Morgan Hill, California, earthquake, which occurred on the Calaveras fault. They also take the additional step of constructing a fully dynamic model that fits the seismic waveform data. Thus, a common picture emerges for earthquakes on strike-slip faults with high geological slip rates (Morgan Hill), strike-slip faults with low slip rates (Landers, Kobe), and thrust faults (Northridge), and for event magnitudes (M_w) ranging from 6.2 (Morgan Hill) to 7.3 (Landers).

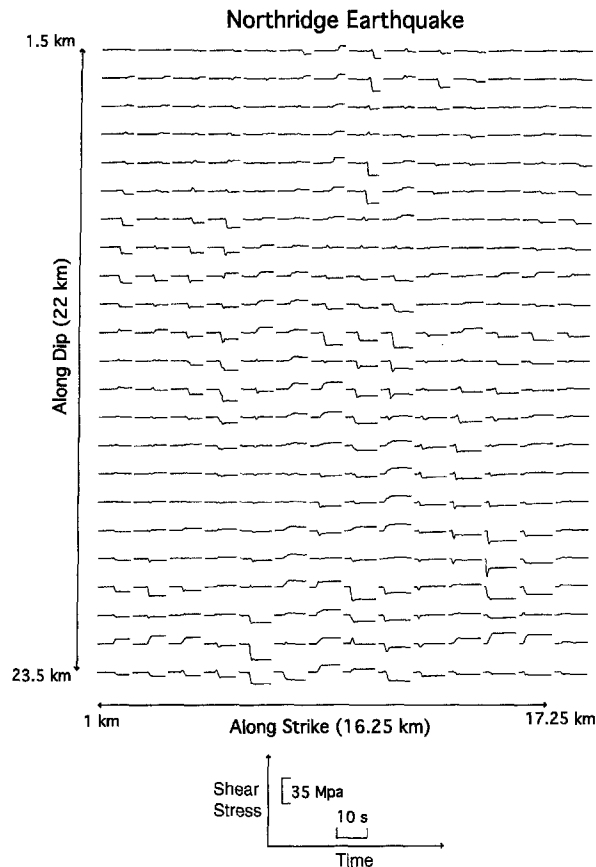


Figure 5. Time histories of shear change on the fault plane of the Northridge earthquake. The left edge of each curve is positioned at the fault plane point to which it corresponds.

If the resolution of the kinematic models were ideal, then the procedures followed here would have provided us with precise images of the fault-zone constitutive equations, that is, shear stress as a functional of the local slip history [Ide and Takeo (1997) present their similar analysis in that form]. In that idealized case, we would be able to claim to have ruled out the self-healing hypothesis as the predominant mechanism controlling slip duration on the basis of these results. This is not the case, however. Due to the limited spatial and temporal resolution of the kinematic models from which we started, we cannot rule out self-healing behavior over shorter, unresolved timescales. Thus, our only claims are that (1) the self-healing hypothesis currently lacks positive evidence from seismic waveform inversions, and (2) if the mechanism does play a significant role in fault dynamics, it must act over timescales shorter than those resolved by the kinematic models, with characteristic times less than perhaps 1 or 2 sec. In fact, since there will always be limits to the attainable temporal resolution of seismic waveform inversions, it may always be impossible to completely rule out the self-healing hypothesis on the basis of seismic (and geodetic) displacement fields alone.

The stress drop in the patches of high slip in these kinematic models is usually spread out over most of the duration of slip, rather than occurring abruptly at the rupture front. This is evident in Figure 7, which shows some examples of shear stress change versus slip (displacement), from the Landers LJV segment. This apparently gradual stress drop is most likely an artifact of the limited time resolution of the kinematic models. Again, if we had ideal resolution, curves such as those in Figure 7 could be interpreted as images of the slip-weakening breakdown process in the rupture zone. In fact, however, it is quite likely that the smoothness of the stress drop is a reflection of our limited resolution. Ironically, rather than being too short, the slip durations in these models could actually be even more concentrated at the rupture front and be consistent with cracklike behavior.

The limited resolution of the kinematic inversions is probably also responsible for the lack of any strong transient stress increases ahead of the rupture front in our shear stress reconstructions. Although transient stress increases of a few tens of percent of the stress drop are evident prior to rupture in a few locations (e.g., left edge of Landers HV segment, Fig. 4b; near-surface locations on the Landers CE segment, Fig. 4c), any inferred prerupture stress increases are usually very small, just a few percent of the stress drop. This result is congruent with the smoothed imaging of the stress drops that was just noted. Apparently, the temporal smoothing of the stress drop that resulted from the limited temporal resolution of the kinematic inversion has nearly eliminated our ability to image the short-duration, prerupture stress concentrations characteristic of rupture propagation.

As we pointed out earlier, the self-healing and geometrical constraint models should be viewed as end-member models, and actual fault behavior may combine elements of both. Indeed, Cochard and Madariaga (1994, 1996) have found that rate-dependent friction only induces narrow slip pulses when combined with heterogeneity of prestress. In their simulations, although the rate-dependent friction law is self-healing, it is the dimension of the initial stress concentration that actually controls the dimension of the slip pulse. If rate-dependent effects on shear stress are partially masked by effects of initial stress heterogeneity, then observational detection of rate-dependent fault friction may be significantly more difficult than suggested by the simplified conceptual picture in Figure 2.

If evidence of self-healing fault-zone rheology can eventually be established, it would provide an important constraint on the physical processes resisting earthquake slip. Such evidence might provide a key clue to the resolution of the heat flow paradox (i.e., the apparently very low dynamic shear stresses resisting slip during earthquakes, at least during the dominant moment-release events on the San Andreas fault). Given its potential significance, the hypothesis deserves continued observational testing.

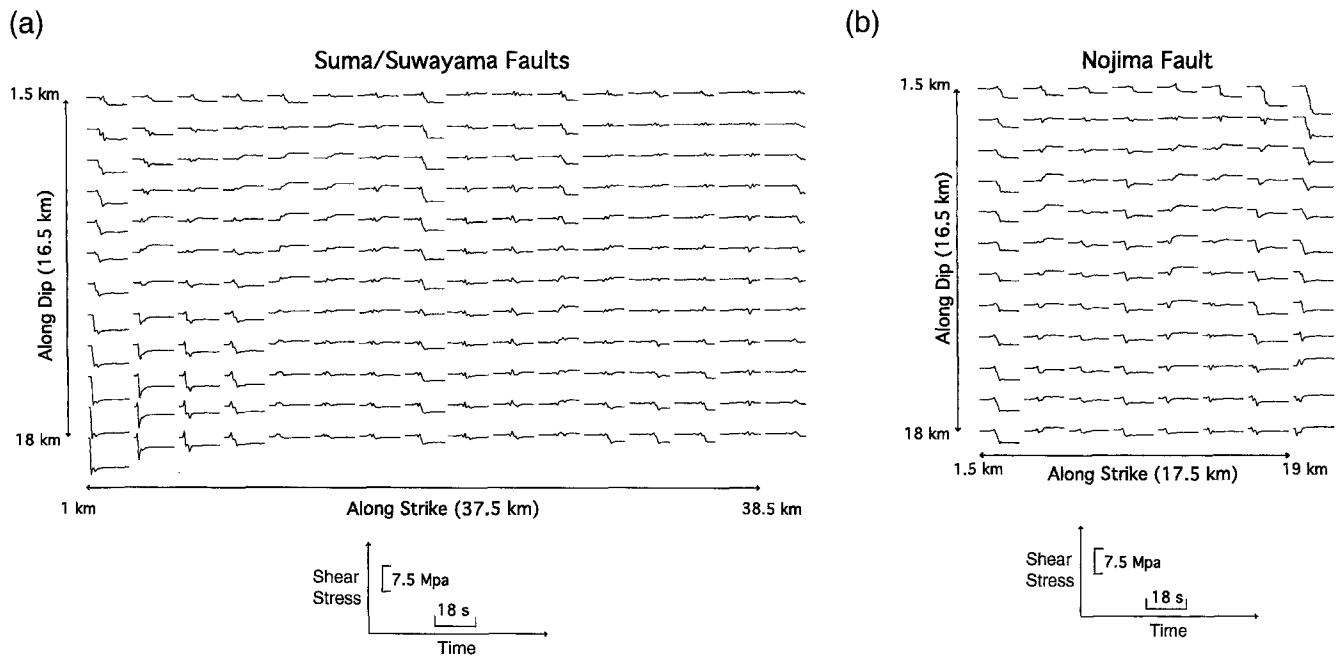


Figure 6. Time histories of shear stress change on the fault planes of the Kobe earthquake. The left edge of each curve is positioned at the fault plane point to which it corresponds. (a) Suma/Suwayama segment. (b) Nojima segment.

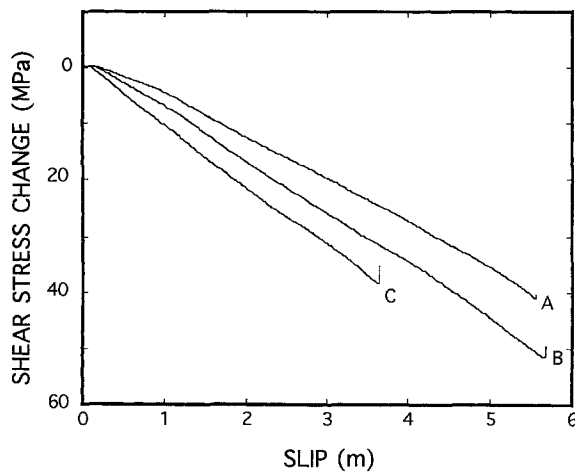


Figure 7. Shear stress change versus slip for three points on the Landers/Johnson Valley segment of the Landers earthquake. The curves are labeled in correspondence with the labeled points in Figure 4a.

Conclusions

Dynamic shear stress changes for the 1992 Landers, 1994 Northridge, and 1995 Kobe earthquakes are consistent with the geometrical constraint model, in which short duration of slip is attributed to spatial heterogeneity of stress drop and, consequently, rapid equilibration of the elastic stress field with the residual dynamic friction level. The self-healing hypothesis, which assumes that rapid dynamic re-strengthening occurs at some distance behind the rupture front, appears to be unnecessary to explain the observed slip

durations in the three earthquakes analyzed. The kinematic models upon which the analysis is based have limited spatial and temporal resolution, and therefore, we cannot rule out the possibility that a self-healing rheology operates on some shorter, unresolved timescale, with characteristic time less than 1 to 2 sec. However, there is little independent empirical evidence for such a fault-zone rheology. This hypothesis about fault dynamics has been proposed primarily on the basis of fault kinematic images, which, we have shown, do not in fact require it. In contrast, the same kinematic models do imply strong heterogeneity of stress drop, with stress-drop concentrations that are highly confined spatially, as required to explain short slip durations under the geometrical constraint hypothesis. Combining our analysis with related, independent investigations, we find similar results for strike-slip faults with high geological slip rates, strike-slip faults with low slip rates, and thrust faults, and for event magnitudes (M_w) ranging from 6.2 to 7.3. Thus, we conclude that friction laws with strong velocity dependence at high slip rate, or other self-healing properties, are at this time unnecessary constructs for interpreting fault kinematics.

Acknowledgments

This work was supported by grants from the U.S. Geological Survey and the Southern California Earthquake Center (SCEC), as well as by a SCEC postdoctoral fellowship (to Yu Guang). We benefited from the suggestions of Raul Madariaga, Satoshi Ide, Michael Fehler, and an anonymous reviewer. This work was undertaken in part while one of the authors (S. Day) was a Visiting Scholar at the Institute of Geophysics and Planetary Physics of the University of California, San Diego. This is SCEC Contribution Number 374.

References

- Andrews, D. J. (1976). Rupture propagation with finite stress in antiplane strain, *J. Geophys. Res.* **81**, 3575–3582.
- Andrews, D. J. and Y. Ben-Zion (1996). Wrinkle-like slip pulse on a fault between different materials, *J. Geophys. Res.* **102**, 553–571.
- Archuleta, R. J. (1984). A faulting model for the 1979 Imperial Valley earthquake, *J. Geophys. Res.* **89**, 4559–4585.
- Archuleta, R. J. and S. M. Day (1980). Dynamic rupture in a layered medium: the 1966 Parkfield earthquake, *Bull. Seism. Soc. Am.* **70**, 671–689.
- Beeler, N. M. and T. E. Tullis (1996). Self-healing slip pulses in dynamic rupture models due to velocity-dependent strength, *Bull. Seism. Soc. Am.* **86**, 1130–1148.
- Beroza, G. C. and T. Mikumo (1996). Short slip duration in dynamic rupture in the presence of heterogeneous fault properties, *J. Geophys. Res.* **101**, 22449–22460.
- Beroza, G. C. and P. Spudich (1988). Linearized inversion for fault rupture behavior: application to the 1984 Morgan Hill, California, earthquake, *J. Geophys. Res.* **93**, 6275–6296.
- Bouchon, Michel (1997). The state of stress on some faults of the San Andreas system as inferred from near-field strong motion data, *J. Geophys. Res.* **102**, 11731–11744.
- Brune, J. N., S. Brown, and P. A. Johnson (1993). Rupture mechanism and interface separation in foam rubber models of earthquakes: a possible solution to the heat flow paradox and the paradox of large overthrusts, *Tectonophysics* **218**, 59–67.
- Cochard, A. and R. Madariaga (1994). Dynamic faulting under rate-dependent friction, *Pure Appl. Geophys.* **142**, 419–445.
- Cochard, A. and R. Madariaga (1996). Complexity of seismicity due to highly rate-dependent friction, *J. Geophys. Res.* **101**, 25321–25336.
- Cotton, F. and M. Campillo (1995). Frequency domain inversion of strong motions: application to the 1992 Landers earthquake, *J. Geophys. Res.* **100**, 3961–3975.
- Day, S. M. (1982a). Three-dimensional simulation of spontaneous rupture: the effect of nonuniform prestress, *Bull. Seism. Soc. Am.* **72**, 1881–1902.
- Day, S. M. (1982b). Three-dimensional finite difference simulation of fault dynamics: rectangular faults with fixed rupture velocity, *Bull. Seism. Soc. Am.* **72**, 705–727.
- Dieterich, J. H. (1981). Potential for geophysical experiments in large scale tests, *Geophys. Res. Lett.* **8**, 653–656.
- Fukuyama, E. and R. Madariaga (1995). Integral equation method for plane crack with arbitrary shape in 3D elastic medium, *Bull. Seism. Soc. Am.* **85**, 614–628.
- Fukuyama, E. and T. Mikumo (1993). Dynamic rupture analysis: inversion for the source process of the 1990 Izu-Oshima, Japan, earthquake ($M = 6.5$), *J. Geophys. Res.* **98**, 6529–6542.
- Harris, R. A. and S. M. Day (1993). Dynamics of fault interaction: parallel strike-slip faults, *J. Geophys. Res.* **98**, 4461–4472.
- Harris, R. A. and S. M. Day (1997). Effects of a low-velocity zone on a dynamic rupture, *Bull. Seism. Soc. Am.* **87**, 1267–1280.
- Harris, R. A., R. J. Archuleta, and S. M. Day (1991). Fault steps and the dynamic rupture process: 2-D numerical simulations of a spontaneously propagating shear fracture, *Geophys. Res. Lett.* **18**, 893–896.
- Hartzell, S. H. and T. H. Heaton (1983). Inversion of strong-ground motion and teleseismic waveform data for the fault rupture history of the 1979 Imperial Valley, California earthquake, *Bull. Seism. Soc. Am.* **73**, 1553–1583.
- Hartzell, S., P. Liu, and C. Mendoza (1996). The 1994 Northridge, California, earthquake: investigation of rupture velocity, risetime, and high-frequency radiation, *J. Geophys. Res.* **101**, 20091–20108.
- Heaton, T. H. (1990). Evidence for and implications of self-healing pulses of slip in earthquake rupture, *Phys. Earthquake Planet. Interiors* **64**, 1–20.
- Ida, Y. (1972). Cohesive force across the tip of longitudinal-shear crack and Griffith's specific surface energy, *J. Geophys. Res.* **77**, 3796–3805.
- Ide, S. and M. Takeo (1997). Determination of constitutive relations of fault slip based on seismic wave analysis, *J. Geophys. Res.* **102**, 27379–27391.
- Lachenbruch, A. H. (1980). Frictional heating, fluid pressure, and the resistance to fault motion, *J. Geophys. Res.* **85**, 6097–6112.
- Madariaga, R. (1976). Dynamics of an expanding circular fault, *Bull. Seism. Soc. Am.* **66**, 639–666.
- Melosh, H. J. (1979). Acoustic fluidization: a new geological process? *J. Geophys. Res.* **84**, 7513–7520.
- Mikumo, T. (1994). Dynamic fault rupture processes of moderate-size earthquakes inferred from the results of kinematic waveform inversion, *Ann. Geofis.* **XXXVII**, 1377–1389.
- Mikumo, T. and T. Miyatake (1995). Heterogeneous distribution of dynamic stress drop and relative fault strength recovered from the results of waveform inversion: the 1984 Morgan Hill, California, earthquake, *Bull. Seism. Soc. Am.* **85**, 178–193.
- Ohnaka, M. and Y. Kuwahara (1990). Characteristic features of local breakdown near crack-tip in the transition zone from nucleation to dynamic rupture during stick-slip shear failure, *Tectonophysics* **175**, 197–220.
- Olson, A. H. and R. Apsel (1982). Finite faults and inverse theory with applications to the 1979 Imperial Valley earthquake, *Bull. Seism. Soc. Am.* **72**, 1969–2002.
- Perrin, G., J. R. Rice, and G. Zheng (1996). Self-healing slip pulse on a frictional surface, *J. Mech. Phys. Solids* **43**, 1461–1495.
- Rice, J. R. (1996). Elastodynamic simulations of rupture propagation and earthquake sequences along complex fault systems, in Southern California Earthquake Center Annual Report for 1996, Vol II.
- Sibson, R. H. (1973). Interactions between temperature and pore-fluid pressure during earthquake faulting: a mechanism for partial or total stress relief, *Nature* **243**, 66–68.
- Wald, D. (1996). Slip history of the 1995 Kobe, Japan, earthquake determined from strong motion, teleseismic, and geodetic data, *J. Phys. Earth* **44**, 489–504.
- Wald, D. J. and T. H. Heaton (1994). Spatial and temporal distribution of slip for the 1992 Landers, California, earthquake, *Bull. Seism. Soc. Am.* **84**, 668–691.
- Wald, D., T. H. Heaton, and K. W. Hudnut (1996). The slip history of the 1994 Northridge, California, earthquake determined from strong-motion, teleseismic, GPS, and leveling data, *Bull. Seism. Soc. Am.* **86**, S49–S70.
- Zeng, Y. and J. G. Anderson (1996). A composite source modeling of the 1994 Northridge earthquake using genetic algorithm, *Bull. Seism. Soc. Am.* **86**, S71–S83.

Department of Geological Sciences
San Diego State University
San Diego, California 92182
(S.M.D., G.Y.)

U.S. Geological Survey
525 South Wilson Avenue
Pasadena, California 91106
(D.J.W.)